Volume 12, Number 4 (August 2019) p. 738 – 765 • ISSN 1983-4195
http://dx.doi.org/10.1590/S1983-41952019000400003

REVISTA IBRACON DE ESTRUTURAS E MATERIAIS
IBRACON STRUCTURES AND MATERIALS JOURNAL

Flexural behavior of hybrid GFRP – concrete railway sleepers

Comportamento à flexão de dormentes ferroviários híbridos de GFRP – concreto

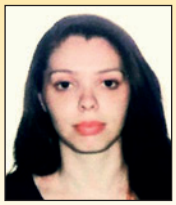

A. C. L. DE AZEVEDO [a]
carollopesazevedo@gmail.com
https://orcid.org/0000-0002-3777-8241

A. M. A. J. TEXEIRA [a]
anam@ime.eb.br
https://orcid.org/0000-0003-3762-7192

L. A. V. CARNEIRO [b]
luizcarneiro@id.uff.br
https://orcid.org/0000-0001-7036-2048

Abstract

This paper aims to present the flexural behavior of hybrid GFRP (glass fiber reinforced polymer) concrete beams as sleepers to railway application. It was tried to obtain sleepers with adequate mechanical resistance, not susceptible to corrosion, durable and lighter than the sleepers in prestressed concrete. Pultruded fiberglass and polyester resin profiles were filled with high strength concrete and polyolefin fiber in the following proportions by volume: 1% and 2.5%. The beams were 1.06 meters long and had a 76 mm x 76 mm x 6 mm cross section, corresponding to a reduced model in a 1: 2.64 scale of a 2.80 meters long sleeper. In the bending tests, the load was applied at the center of the sleeper, as provided in the Brazilian standard NBR 11709 (2015) and American standard AREMA (2016). During the tests the applied load, the vertical deflection and the longitudinal tensile and compression deformations were measured in the center of the span. The influence of fiber addition on the strength, rupture mode and flexural modulus of elasticity of the hybrid beams was analyzed. Finally, the hybrid sleeper performance was compared to that of the prestressed concrete monoblock sleeper. The results obtained were satisfactory, indicating that the proposed hybrid sleeper is a constructively and technically feasible alternative.

Keywords: sleeper, concrete, GRFP, polyolefin fiber, experimental analysis.

Resumo

Este trabalho tem por objetivo apresentar o comportamento à flexão de vigas híbridas de GFRP (glass fiber reinforced polymer – polímero reforçado com fibra de vidro) e concreto para aplicação em dormentes ferroviários. Pretendeu-se obter dormentes com adequada resistência mecânica, não susceptíveis à corrosão, duráveis e mais leves que os dormentes em concreto protendido. Foram estudados perfis pultrudados de fibra de vidro e resina de poliéster, preenchidos com concreto de alta resistência e fibras de poliolefina nas seguintes proporções em volume: 1% e 2,5%. As vigas tinham 1,06 metros de comprimento e seção transversal de 76 mm x 76 mm x 6,2 mm, correspondendo a um modelo reduzido em escala 1 : 2,64 de um dormente de 2,80 metros de comprimento. Nos ensaios de flexão, a carga foi aplicada no centro do dormente, conforme previsto nas normas ABNT NBR 11709 (2015) e AREMA (2016). Durante os ensaios foram medidas a carga aplicada, a flecha e as deformações longitudinais de tração e compressão no centro do vão. Foi analisada a influência da adição de fibras na capacidade resistente, no modo de ruptura e no módulo de elasticidade à flexão das vigas híbridas. Por fim, o desempenho do dormente híbrido foi comparado ao do dormente monobloco em concreto protendido. Os resultados obtidos foram satisfatórios, indicando que o dormente híbrido proposto é uma alternativa viável construtivamente e tecnicamente.

Palavras-chave: dormente, concreto, GFRP, fibra de poliolefina, análise experimental.

[a] *Instituto Militar de Engenharia, Seção de Engenharia de Fortificação e Construção, Rio de Janeiro, RJ, Brasil;*
[b] *Universidade Federal Fluminense, Departamento de Engenharia Civil, Niterói, RJ, Brasil.*

Received: 20 Sep 2017 • Accepted: 16 Aug 2018 • Available Online: 08 Aug 2019

1. Introduction

The sleepers are elements that are positioned at the transverse direction of the axis of the pathway, on which the rails are placed. With the fixture system, they constitute the union element between the ballast and the rail, forming with this the structure of the pathway. The dimensions of the sleeper vary according with the use and the track gauge. The known track gauges are: the broad gauge with 1.60 meters, more used in Brazil, the standard gauge with 1.435 meters and the narrow gauge with 1.00 meter, as shown in Figure 1 (Planeta Ferrovia [1]).

First railways adopted sleepers made of wood (see Figure 2), because this is a material with high mechanical strength and flexibility, which results in a great capacity to withstand the vibrations from the dynamic actions acting on the permanent track (Bastos [2]). Over the years, however, there were disadvantages in the use of wood sleepers, such as: scarcity of noble wood and high need for wood replacement due to time and biological agents, leading to the need to search new technologies. From the Second World War, the countries of Europe, mainly England, France and Germany, began to replace the wooden sleepers by the concrete sleepers (Bastos [2]).

Concrete sleepers can be classified as mono-block or bi-block elements as shown in Figure 3. Bi-block sleepers are reinforced concrete elements interconnected by a metallic profile. The mono-block sleepers are of prestressed concrete because, in general, the tests carried out with reinforced concrete sleepers led to unsatisfactory results. An exception is the reinforced concrete mono-block sleeper designed by Eternit, in Italy, which used cement with asbestos fibers (Bastos [2]). Mono-block sleepers resist higher loads than the bi-block sleepers and have high durability to time and biological agents. However, they are very robust and heavy, usually more than 400 kg mass. Therefore, it is necessary to use heavy machinery for the transportation and installation of these sleepers. Besides, the construction and the demobilization costs of sleeper factory near the railway site are quite high.

The steel sleepers have longer service life than the wood sleepers, high mechanical resistance and are lightweight (around 70 kg mass) (Trindade [3]). According to DNIT [4], the steel sleepers are easy to settle, but their lightweight is inconvenient for heavy traffic lines. The steel sleepers also have low corrosion resistance, requiring proper treatment for its mitigation. They are also electrical conductors, requiring the installation of insulation in the rail/sleeper interface.

This work presents and analyzes test results of pultruded glass fiber reinforced polymer (GFRP) sleepers filled with concrete, without or with polyolefin fibers addition to the mass, in a reduced model with 1.06 meters length. The authors also extrapolate the experimental results for a prototype of 2.80 meters length and compared their resistance capacity and their weight with that of a mono-block prestressed concrete sleeper, usually adopted in Brazilian railways.

The association between concrete and pultruded glass fiber polymer profile aims to reduce or even eliminate the main problems of the railway sleepers, which are: the high weight in the case of sleepers in concrete, corrosion susceptibility in the case of steel sleepers and low resistance to biological agents in the case of wood sleepers. The addition of polyolefin fibers to the concrete is intended to increase the resistance to the traction and to delay the opening of cracks. Polyolefin fiber is not subject to corrosion

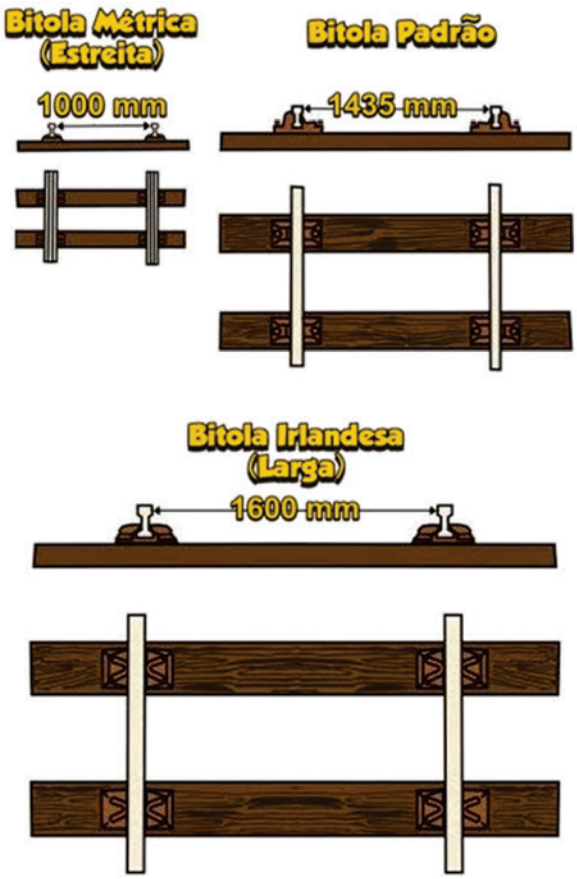

Figure 1
Most used railway gauge, Revista Ferroviária [1]

Figure 2
Wood sleeper, Mundo dos Trilhos [20]

and is lighter than steel fiber, whose addition to concrete is already widespread worldwide.

Research found in the literature on the Association of Concrete to the Pultrudado profile of fiberglass and resin for application in beams and research on the addition of polyolefin fibers to the concrete are presented below.

2. Theoretical reference

2.1 Fiber reinforced polymer

The fiber reinforced polymer is a composite material formed by combining two materials, one being the reinforcement in synthetic fibers and the other the polymer matrix. The combination of materials enables the composite to achieve properties that individually the materials would not reach. (Gibson [5])

The main synthetic fibers are glass, carbon and aramid. The glass fibers are the cheapest and therefore the most used fibers in the manufacture of composite materials. There are several processes of manufacturing composite materials among which stands out the pultrusion. Such process gives the product distinct characteristics, therefore, the quantity and orientation of the fibers have influence on the physical and mechanical properties of the composite material and its production cost. The pultrusion enables the fabrication of constant cross-section profiles. It consists of the "pulling" of resin-impregnated fibers, through a heated metallic mold, producing profiles with high mechanical properties in the direction of the fibers, at a low cost and immune to corrosion.

2.2 Association between pultruded profiles and concrete for application in beams

Studies proposing the association between pultruded profiles and concrete for application in beams were recently published and come arousing the interest of researchers and companies. Ferdous *et al.* [6] investigated the feasibility of applying a hybrid beam of pultruded GFRP and geopolymeric concrete as sleepers for railways. The compressive characteristic strength of the geopolymeric concrete and the Portland cement concrete were, respectively, 40 MPa and 57 MPa. The square tubular profiles had dimensions of 190 mm x 100 mm x 10 mm x 2000 mm long. The experimental and computer simulation results obtained showed that the rupture of the hybrid beam occurred due to the crushing of the concrete in the compressed region. The vertical displacement results and the pressure on the ballast of the sleeper were similar to those obtained in traditional wood sleepers, which increases the possibility of acceptance of this type of sleeper in light rail transport.

Muttashar *et al.* [7] also studied the influence of the concrete on the bending of hybrid beams formed by concrete-filled pultruded GFRP square tubes. The GFRP profiles had dimensions of 125 mm x 125mm x 6.5 mm x 2000 mm long filled with concretes with average compressive strength of 10 MPa, 37.5 MPa and 43.5 MPa. They verified that the concrete-filled profiles resisted a load 100% to 140% higher than the hollow profiles and had a 25% increase in rigidity. The increase in the compression strength of concretes (from 10 MPa to 43.5 MPa) increased the failure load by 19% and practically did not change the flexural stiffness of the beam.

Muttashar *et al.* [8] studied the bending behavior of multicellular pultruded GFRP beams filled partially with concrete. For this, they glued GFRP square tubes with dimensions of 125 mm x 125 mm x 6.5 mm with epoxy adhesives, forming beams with one to four cells, with lengths of 2000 mm (single-cell), 2750 mm (two cells), 3700 mm (three cells) and 5000 mm (four cells). The authors used concretes with compression resistances of 15 MPa and 32 MPa to fill the upper cell of the multicellular beams. The beams were tested in bending and their behaviors were compared to those of hollow beams. The results showed an increase of up to 27% in the resistance of the multicellular beams when compared to the beams

(a) (b)

Figure 3
Pathway: (a) mono-block sleeper, PANDROL [21] e (b) bi-block sleeper, Revista Ferroviária [1]

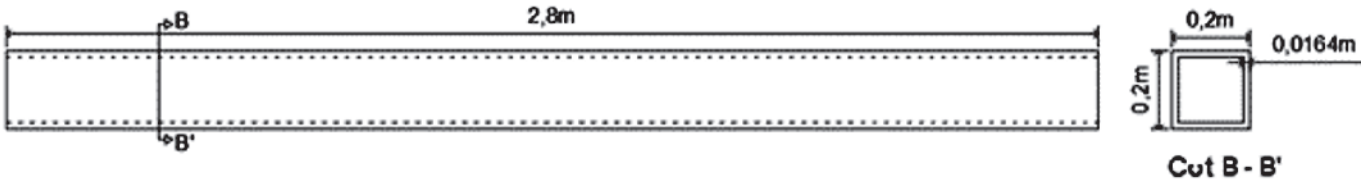

Figure 4
Longitudinal view and cross section of the prototype GFRP (Author)

of a single cell. The filling of the upper cell of the beams with concrete increased the load capacity and the stiffness of the beams. The multicellular GFRP beams filled with concrete in the upper cell failured with 38% to 80% higher load and presented 10% to 22% higher stiffness than the corresponding hollow multicellular beams. The increase in the concrete compression strength of the beams, from 15 MPa to 32 MPa, resulted in an increase of up to 14% in the failure load.

2.3 Addition of polyolefin fiber to concrete

Gaspar, Carneiro and Teixeira [9] studied the addition of steel fiber and polyolefin fiber in concretes subjected to ballistic impact. The authors tested 28 square plates with dimensions of 300 mm x 150 mm. 14 plates were molded with conventional concrete resistance and 14 other plates were molded with high-strength concrete. The volumetric contents of fibers were 0%, 0.5%, 1.0% and 1.5%. For the ballistic test 7.62 mm caliber projectiles were used to check the shielding capacity and the level of damage on each concrete plate. The results indicated that the addition of steel fibers and polyolefin fibers favored the increase of the initial concrete compressive strength, the shielding capacity and the reduction of damage caused by the impact.

Alberti *et al.* [10] and Alberti *et al.* [11] studied the difference in the orientation and density of polyolefin fibers added to the mechanical vibrated concrete and self-consolidating concrete. Fibers with 60 mm and 48 mm long were added to the concrete in the proportion of 9 kg/m^3, which is equivalent to 1.0% in volume. Samples with dimensions of 150 mm x 150 mm x 600 mm were molded and tested in bending. The concrete characteristic compressive strength varied from 32.9 MPa to 39.3 MPa. The self-consolidating concrete samples presented more uniform distribution of the fibers, as well as the samples with fibers of 48 mm long showed better orientations. The authors concluded that polyolefin fibers can meet the requirements of the standards, contributing in reducing the post-pick load cracking of the structural element. They also verified that while the length of the fiber, the type of concrete and the sample dimensions influence the fracture surface, the positioning and orientation of the fibers throughout the piece can be quite relevant on the performance of the structural element.

3. Materials and methods

3.1 Sleeper design

The design of a sleeper must meet the requirements of the technical standards. The specific Brazilian standard for concrete sleepers is the ABNT NBR 11709 [12]. ABNTs design methodology [12] it's very similar to AREMA [13]. This is because the characteristics of the Brazilian pathways, with regard to the type of transport and the quality of maintenance, are similar to the American pathways. The design methodology of ERRI, described in CEN (1996), leads to lighter and less resistant sleepers than the sleepers designed according to the American standard. (Bastos [2])

3.2 Sleeper prototype design

The sleeper prototype is composed of a pultruded GFRP square tube filled with concrete with average compressive strength of 73 MPa. Considering the dimensions of the shoulder pads of the prestressed concrete sleeper, profiles with 200 mm x 200 mm x 16.4 mm was chosen, as presented in Figure 4. The length of 2.80 meters is usual for prestressed concrete sleeper in Brazil, so it was adopted in this project. Figure 5 shows the schematic design of the GFRP /concrete hybrid sleeper. It should be emphasized that, according to ABNT NBR 11709 [12], the concrete characteristic compression strength of sleepers may not be less than 45 MPa.

GFRP present high tensile strength in the direction of the fibers and low specific weight. The GFRP filled with concrete aims to increase the stiffness and the resistance to bending and shear of the beam. Therefore, the association between the GFRP and concrete can be a good alternative to obtain mono-block

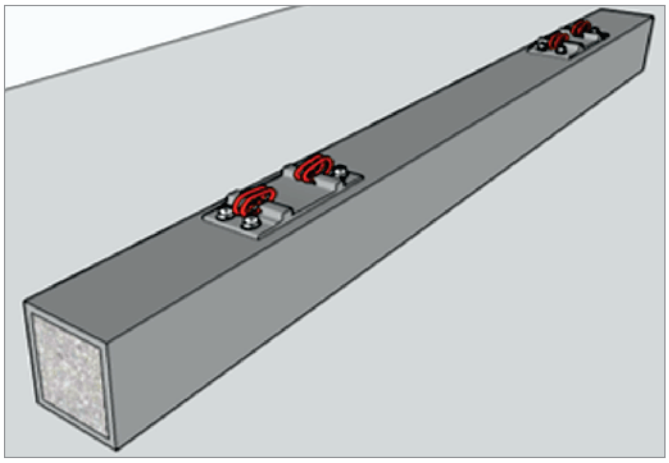

Figure 5
Schematic drawing of GFRP/concrete hybrid sleeper (Author)

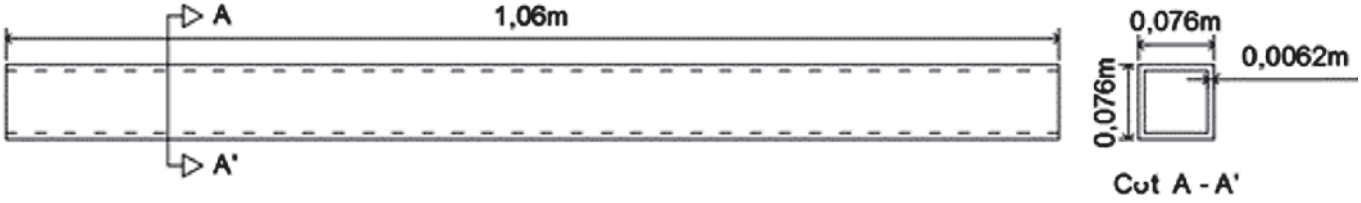

Figure 6
Longitudinal view and cross section of the GFRP profile of the reduced model (Author)

sleepers lighter than the prestressed concrete mono-block sleepers. The GFRP square tubes are usually manufactured and traded in the Brazilian market, but with transverse section dimensions smaller than 200 mm x 200 mm. Therefore, it was decided to study a reduced model of the sleeper, using the profiles dimensions available in the market.

3.2 Reduced sleeper model design

For the design of the reduced sleeper model, the theory of the similarity of the physical models was applied, which allows a reduced model of structure to reproduce the behavior of the prototype. For this, the dimensional analysis of the deformation problem was done according to Carneiro [14] and the following representative π numbers were obtained to the problem. This numbers should be equal in the reduced model and in the prototype.

$$\Pi_1 = \frac{F}{El^2} = N_{Ho} \quad (1)$$

$$\Pi_2 = \frac{\gamma l}{E} = N_{Gal.} \quad (2)$$

$$\Pi_3 = \frac{\delta}{l} \quad (3)$$

F is the force applied;
E is the longitudinal Young´s modulus of the material;
l is the length of the sleeper;
γ is the specific weight of the material and
δ is the vertical displacement of the sleeper.
The parameter π_1 is known as Hooke's number. It is applied to materials with linear elastic behavior in which tensions are proportional to deformations, as shown in Teixeira [15]. With the number π_1 and the force in reduced model, the force in the prototype is obtained according to equation (5). As the material of the reduced model is equal to the material of the prototype, it isn't possible to respect directly the number π_2. To attend it indirectly, it is necessary to add mass to the reduced model. So, the specific weight of the prototype (γ_p) is equal to the apparent specific weight of the reduced model (γ_m) multiplied by the relationship between the reduced model length and the prototype length, according to the equation (6). The mass to be added to the reduced model should be equal to $\left(\frac{l_p}{l_m} - 1\right)$ times the mass of the reduced model.
From the number π_3, it is obtained the vertical displacement in the prototype, that is the vertical displacement of the reduced model multiplied by the relationship between the length of the prototype and the length of the reduced model, as shown in equation (4).

$$\delta_p = \frac{\delta_m l_m}{l_p} \quad (4)$$

δ_p is the vertical displacement of the prototype;
δ_m is the vertical displacement of the reduced model;
l_p is the length of the prototype and;
l_m is the length of the reduced model.

$$F_p = \frac{F_m l_p^2}{l_m^2} \quad (5)$$

F_p is the force applied in the prototype and;
F_m is the force applied in the reduced model.

$$\gamma_p = \frac{\gamma_m l_m}{l_p} \quad (6)$$

γ_p is the specific weight of the prototype and;
γ_m is the apparent specific weight of the reduced model.
The scale of the reduced model was defined from the availability of profiles in the Brazilian market. The largest available square profile was adopted, which had 76 mm x 76 mm x 6.2 mm, as shown in Figure 6, resulting in a geometric scale factor between the prototype and the reduced model (lp / lm) of 2.63.
The scale factors of the reduced model in relation to the prototype are presented in Table 1.

Table 1
Scale factors of the reduced model

Magnitude	Scale factor
Vertical displacement	$1/2{,}64$
Profiles area	$1/(2{,}64)^2$
Dead load	$1/(2{,}64)^3$
Applied load	$1/(2{,}64)^2$
Additional mass	1,64

3.4 Experimental program

Seven GFRP/concrete hybrid beams were prepared. Two hybrid beams were of plain concrete, four were of concrete with the addition of 25 mm polyolefin fibers (two with 1% in volume and two with 2.5% in volume) and one beam was of concrete with the addition of 1 % in volume of 35 mm polyolefin fibers.
12 cylindrical concrete samples with dimensions of 150 mm x 300 mm were also concreted. Three samples were of plain concrete, seven

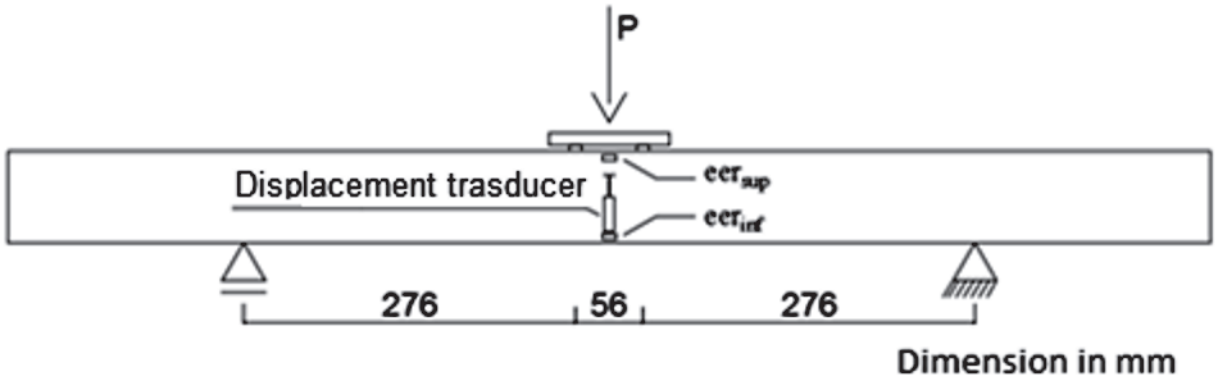

Figure 7
Structural scheme and beam instrumentation (Author)

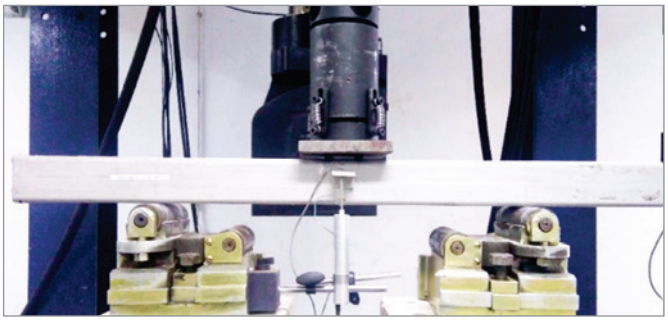

Figure 8
Reduced model of the hybrid sleeper at the beginning of the test (Author)

samples were of concrete with the addition of 25 mm polyolefin fibers (four with 1 % in volume and three with 2.5 % in volume) and two samples were of concrete with 1% addition in volume of 35 mm polyolefin fibers. It was also molded a 100 mm x 200 mm cylindrical sample with 1% addition in volume of 25 mm polyolefin fibers.
14 concrete beams were also molded. Four beams had 1% and four beams had 2.5% addition in volume of 25 mm polyolefin fibers. Three beams were of plain concrete and other three beams had 1% addition in volume of 35 mm polyolefin fibers. All concrete beams were molded with the same length of the reduced model sleeper and with the internal dimensions of the GFRP (63,6 mm x 63,6 mm x 1060 mm).
Samples of GFRP for tensile tests and for determination of the specific weight and the mass fraction of fiber were also prepared.
All the samples and beams were molded and tested at the Building Materials and Concrete Laboratory of the Military Engineering Institute (IME).
The tensile tests of the GFRP samples were carried out in accordance with the ASTM D297 [16] e ASTM D3039/D3039M [17]. The axial compression tests of the cylindrical samples were carried out according to ABNT NBR 5739 standard [18].
The hybrid beams were instrumented with two strain gauges (type KFG-5-120-C1-11 and Kyowa brand) on the upper and lower surfaces of the GFRP profile, in the center of the test span. One displacement transducer with 50 mm course, type DTH-A-50, Kyowa brand, was used to measure the vertical displacement in the center of the span. The structural and instrumentation scheme of the beams is shown in Figure 7.
The hybrid beams were tested in bending and steel rollers were adopted in the supports, as presented in Figure 8. The load was applied at a rate of 22 kN/min with a hydraulic actuator of MTS brand and load capacity of 1000 kN. The acquisition of the loads and the vertical displacements throughout the tests was carried out with the

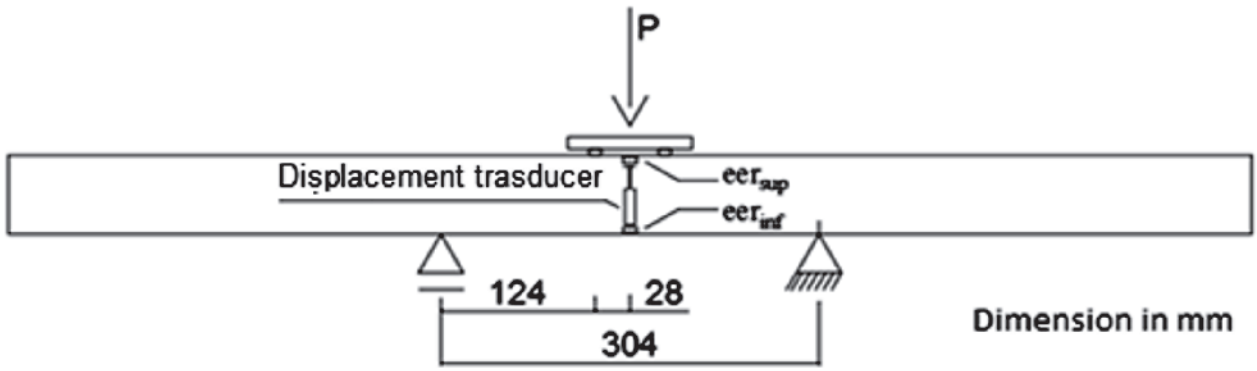

Figure 9
Structural and instrumentation scheme of the concrete beams (Author)

Figure 10
Beam before bending test (Author)

Flextest system, also from MTS brand. The acquisition of the deformations was done with the ADS 2000 system, from Lynx brand. The concrete beams with volumetric variation of fibers were instrumented with two strain gauges (eer_{sup} and eer_{inf}) type KC-80-120-A1 – 11, Kyowa brand, and one displacement transducer, type DTH-A-50 and Kyowa brand, as shown in Figure 9. The beams were tested in bending with a hydraulic actuator of MTS brand and load capacity of 50 kN, as presented in Figure 10. The acquisition of the loads, vertical displacements and deformations were done with the same equipments of the hybrid beams tests.

4. Results and analysis

4.1 Reduced model test results

Table 2 presents the mass fractions of total fibers (V_f total %) and long fibers (V_f long %), the specific weight, the failure strength (σ_{rup}), the failure deformation (ε_{rup}) and the Young's modulus obtained in the tensile tests performed with GFRP samples. The GFRP presents linear behavior and fragile failure.

Table 2
Test results on GFRP samples

Samples	Vf total %	Vf long %	γ (N/m³)	σ_{rup} (MPa)	E (MPa)
Tipo 1	64.12	51.93	18.48	372.01	31614
Tipo 2	64.12	51.93	18.48	447.63	–

Table 3
Concrete compression tests results

% of fiber	CP	Area (mm)	Average failure strength (MPa)	E_{ci} (MPa)
Sem fibras	1	176.7	76.52	33467
	2			–
	3			–
1 – 25 mm	1	176.7	70.40	31702
	2			–
	3			
	4	78.5		–
	5	176.7		30255
2,5 – 25 mm	1	176.7	73.41	–
	2			37252
	3			38678
1 – 35 mm	1	176.7	56.70	32932
	2			27400

Table 3 shows the average failure strength and the Young's modulus of the concrete (plain, with 1% and 2.5% in volume of polyolefin fibers with 25 mm long and 1% in volume of polyolefin fibers with 35 mm, obtained from the compression tests. It is observed that the addition of fibers influenced the compressive strength of the specimens, reducing it. In addition, the failure of the concrete specimens with polyolefin fibers was more ductile than that observed for the plain concrete specimens, as shown in Figure 11 and Figure 12. It can also be observed that the

(a) (b) (c) (d)

Figure 11
Specimens after compression tests: (a) plain, (b) with 1% fibers (25 mm), (c) with 2.5% fibers (25 mm) and 1% fibers (35 mm) (Author)

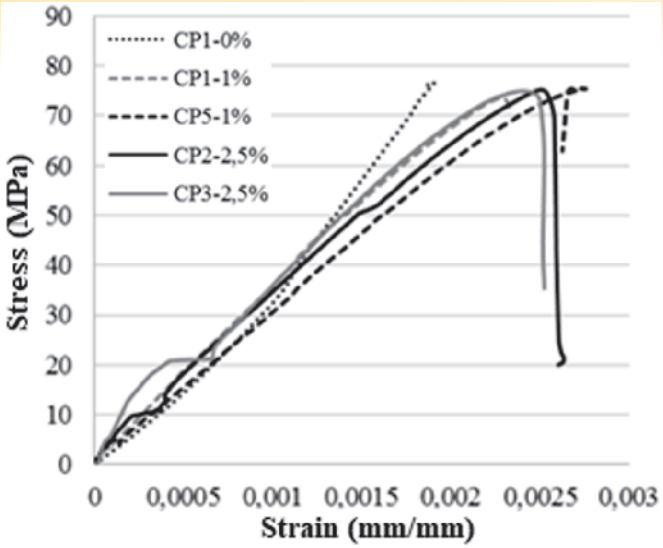

Figure 12
Stress x strain curves of the concrete specimens after compression tests (Author)

compressive strength of the specimens with 1% of fibers of 35 mm was much lower than of the specimens with 1% of fibers of 25 mm. This occurred due to the large number of voids in the specimens (see Figure 11).

Table 4 displays the average failure values of load, vertical displacement and stress (on the upper and lower edges) of the concrete beams and the average compressive and tension failure strength of the corresponding cylindrical concrete samples.

The results of load, vertical displacement and strain (on the upper and lower edges of the GFRP profile) obtained in the hybrid beams tests are presented in the Table 5. The typical failure of the hybrid beam is shown in the Figure 13.

The failure of the hybrid beams occurred on the lower edge and was due to the failure of the concrete by shear followed by the failure of the GFRP profile parallel to the fibers. The smallest failure

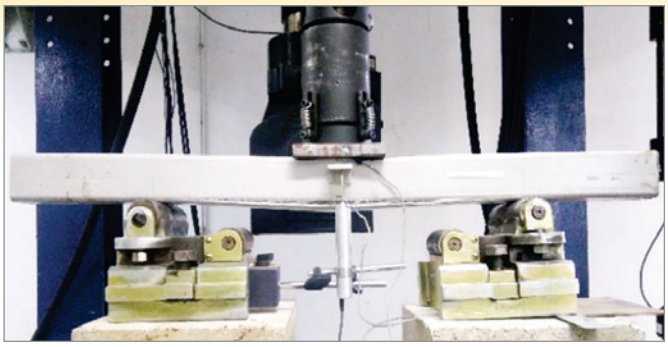

Figure 13
Hybrid sleeper reduced model after failure (Author)

load of the hybrid beam with 1% fibers of 25 mm long is due to the smaller compressive strength of the concrete of these beams.

Figure 14 and Figure 15 present the load x vertical displacement and load x strain curves of the hybrid beams, respectively. All hybrid beams presented similar stiffness, but the beams with added fibers showed greater ductility near the failure.

During the tests a good adherence was observed in the interface GFRP/concrete and the detachment between the profile and the concrete occurred only after the failure of the concrete, culminating in the mode of rupture previously described.

The addition of fibers to the concrete contributed to the increase of the failure load of the hybrid beams, due to the increase of the tensile strength of the concrete. Filling the profile of GFRP with concrete prevented the local buckling of the GFRP webs.

The vertical displacements in the center of the hybrid beams without and with the addition of fibers varied from L/101 (hybrid beams with 1% fibers with 35 mm long) to L/51 (hybrid beams with 1% fibers with 35 mm long), being L the length of the span.

Figure 16 shows the cracking pattern of the concretes with and without fibers of the hybrid beams. It can be noted that the addition of polyolefin fibers reduced the opening of the cracks of the beams with 2.5% in volume of polyolefin fibers with 25 mm long and with 1% in volume of fibers with 35 mm long. Concretes with the

Table 4
Mean values of the concrete beams test results

% of fiber	P_{rup} (kN)	δ_{rup} (mm)	σ_{sup} (MPa)	σ_{inf} (MPa)	f_{cm} (MPa)	$f_{ct,sp}$ (MPa)
0	6.33	0.19	7.23	11.07	76.52	–
1 25 mm	5.89	0.09	7.22	9.94	70.04	–
2.5 25 mm	6.15	0.08	7.53	9.69	73.41	6.11
1 35 mm	6.35	0.31	–	–	50.70	6.08

Table 5
Hybrid beams test results

% of fiber	Beam	P_{rup} (kN)	$P_{rup\ med}$ (kN)	δ_{rup} (mm)	$\varepsilon_{rup\ sup}$ GFRP	$\varepsilon_{rup\ inf}$ GFRP
0	MODRED2	36.92	37.1	6.03	0.0035	0.0046
	MODRED3	37.31		6.35	0.0032	0.0045
1 - 25 mm	MODRED3	37.80	37.5	7.17	0.0039	0.0044
	MODRED4	37.13		7.56	0.0027	0.0038
2,5 - 25 mm	MODRED6	39.14	40.5	7.24	0.0030	0.0055
	MODRED7	41.90		7.61	0.0042	0.0070
1 - 35 mm	MODRED1	39.56	39.6	11.88	0.0023	0.0042

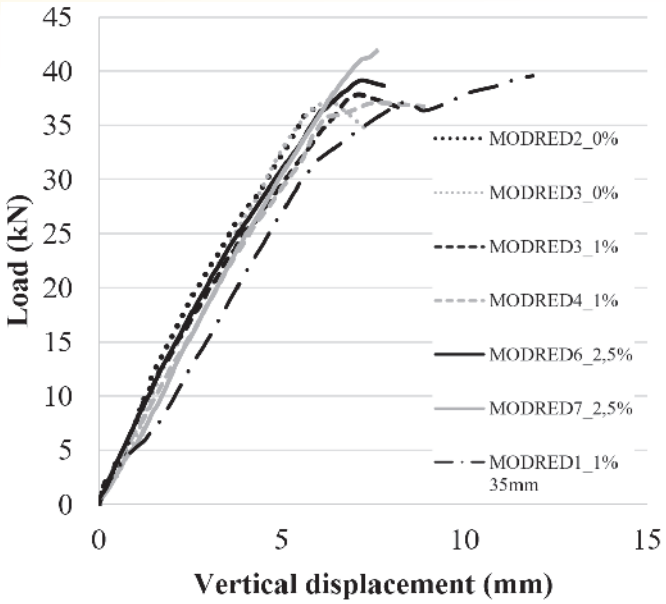

Figure 14
Load x vertical displacement curves of the hybrid beams (Author)

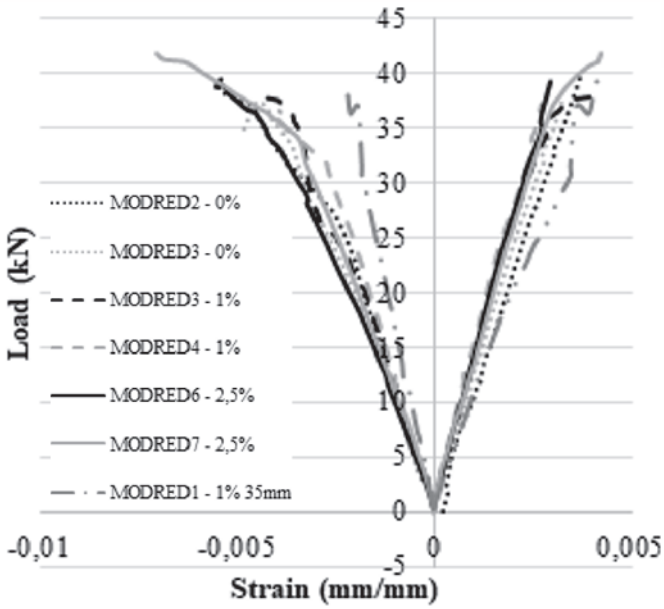

Figure 15
Graph load x strain curves of the hybrid beams (Author)

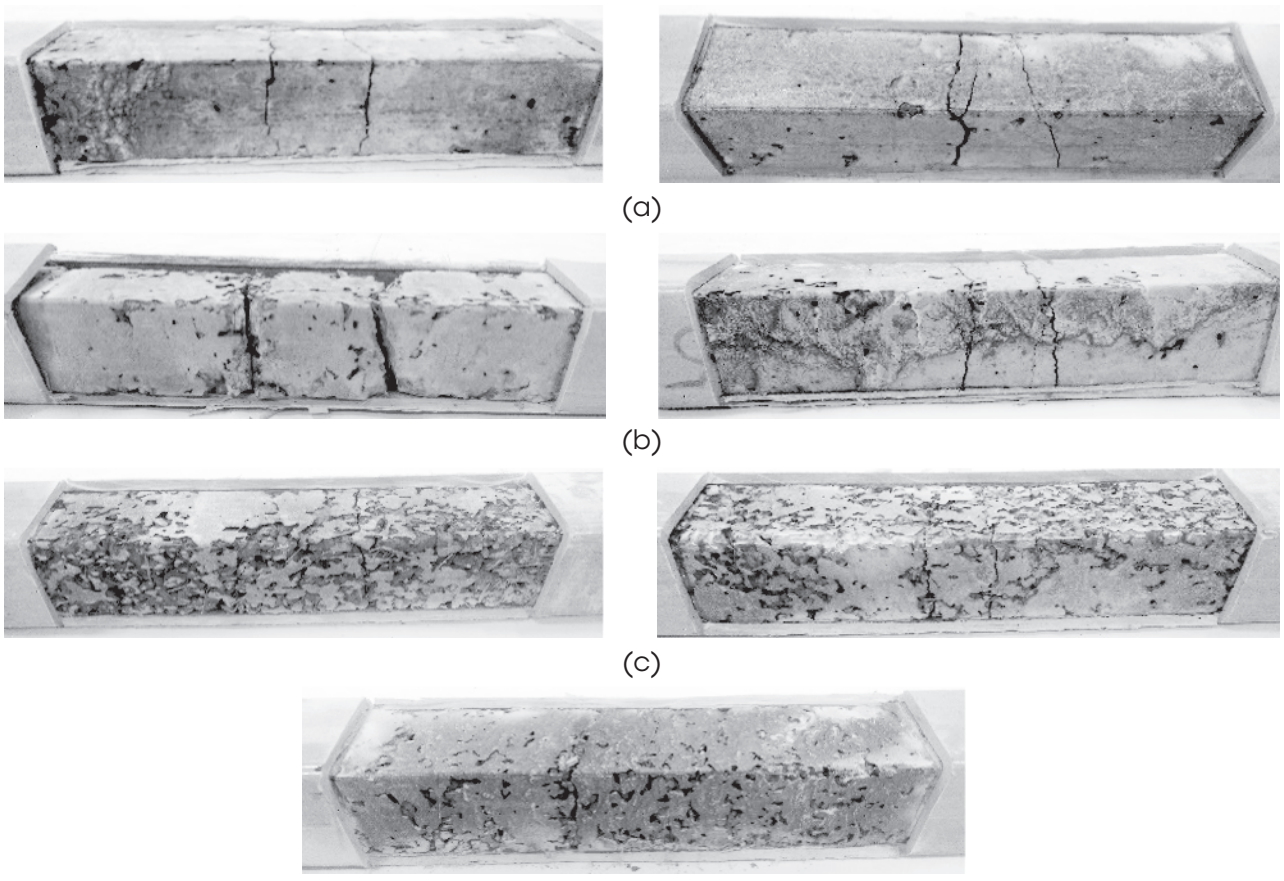

Figure 16
Concrete cracking of the hybrid beams: (a) without fibers, (b) with 1% fiber (25 mm), (c) with 2.5% fiber (25 mm) and (d) with 1% fiber (35 mm) (Author)

Table 6
Hybrid beams stress results

% of fiber	Beam	$\sigma_{rup\ sup}$ GFRP	$\sigma_{rup\ inf}$ GFRP
0	MODRED2	80.80	106.20
	MODRED3	82.03	115.35
1 - 25 mm	MODRED3	80.79	91.15
	MODRED4	81.63	114.89
2,5 - 25 mm	MODRED6	84.23	154.41
	MODRED7	91.53	152.56
1 - 35 mm	MODRED1	85.20	155.58

Table 7
Results calculated from the hybrid beam tests results

% of fiber	Beam	$\varepsilon_{rup\ sup}$ GFRP	$\sigma_{rup\ sup}$ GFRP
0	MODRED2	0.0028	93.70
	MODRED3	0.0026	87.01
1 - 25 mm	MODRED3	0.0032	99.13
	MODRED4	0.0022	68.15
2,5 - 25 mm	MODRED6	0.0023	87.31
	MODRED7	0.0033	125.28
1 - 35 mm	MODRED1	0.0018	54.29

addition of fibers also showed a greater number of voids. In none of the tests occurred the compressed concrete crushing.
A Table 6 displays the normal stress results on the upper and lower edges of the GFRP profile obtained from equation (7) and equation (8), respectively. These stresses were calculated from the bending moment and the neutral line position of the hybrid beam, equation (9), in the mid span section. The position of the neutral line was obtained from the strains of the GFRP profiles measured in the tests, despising the concrete in tension and considering an equivalent homogeneous section of the concrete.

$$\sigma_{supGFRP} = \frac{M.y}{I}.n \quad (7)$$

$\sigma_{sup\ GFRP}$ is the stress on the top edge of the GFRP profile;
M is bending moment;
y is the height of the neutral line;
I is the moment of inertia of the equivalent homogeneous section of the concrete shown in Figure 17;
n is the relationship between the GFRP and concrete Young's modules.

$$\sigma_{infGFRP} = \frac{M.(h-y)}{I}.n \quad (8)$$

$\sigma_{inf\ GFRP}$ is the stress on the bottom edge of the GFRP;
M is bending moment;
y is the height of the neutral line;
h is the height of the profile;
I is the moment of inertia of the homogeneous equivalent section of the concrete shown in Figure 17.

$$y = \frac{\varepsilon_{supGFRP}.b}{\varepsilon_{supGFRP} + \varepsilon_{infGFRP}} \quad (9)$$

y is the height of the neutral line;
$\varepsilon_{supGFRP}$ is strain on the upper edge of the GFRP profile;
b is the width of the GFRP profile;
$\varepsilon_{inf\ GFRP}$ it is strain on the lower edge of the GFRP profile.
Table 7 presents the concrete strain and stress on the upper edge of the concrete in the hybrid beams, calculated according to the equations (10) and (11). It was assumed the perfect adherence between GFRP/concrete and the medium Young's modules obtained in the compressive tests (Table 3), except for the concrete with 1% fibers, in which only one result of Young's modulus was obtained.

$$\varepsilon_{conc} = \frac{\varepsilon_{sup\ GFRP}.(y-e)}{y} \quad (10)$$

ε_{conc} is concrete strain;
$\varepsilon_{sup\ GFRP}$ is strain on the upper edge of the GFRP profile;
y is the height of the neutral line;
e is the thickness of the GFRP profile.

$$\sigma_{conc} = \frac{M.y}{I} \quad (11)$$

σ_{conc} is concrete stress;
M is bending moment;
y is the height of the neutral line;
I is the moment of inertia of the equivalent homogeneous section of the concrete shown in Figure 17.
It is observed that the calculated concrete stresses approached the experiment concrete stresses obtained from the compression tests of cylindrical specimens. The mean tensile stresses on the

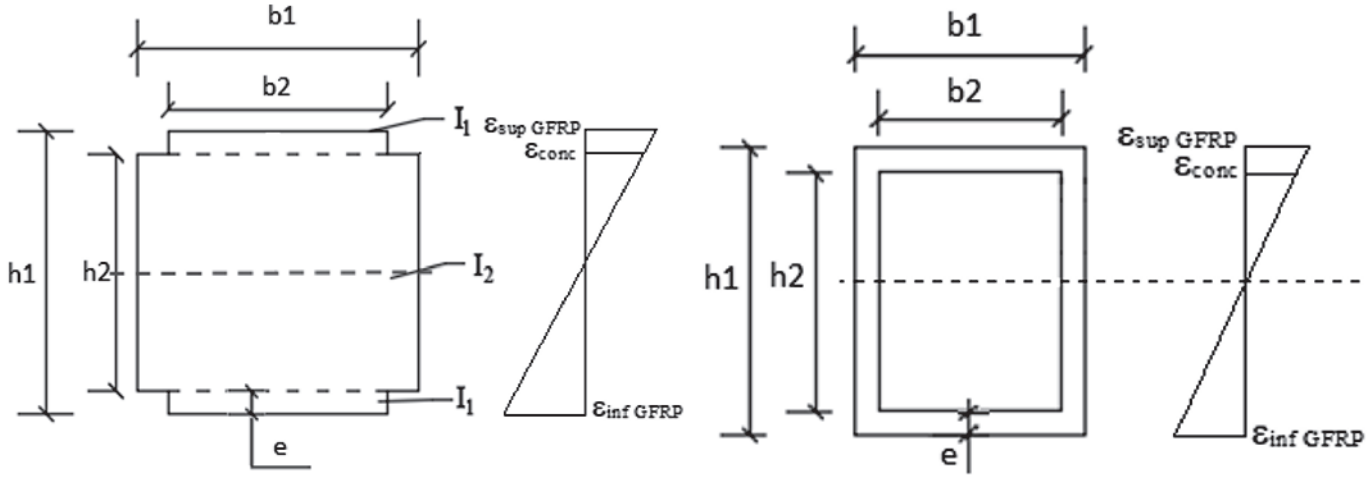

Figure 17
Equivalent homogeneous concrete section (Author)

Table 8
V_C values calculated for each volumetric percentage of fibers

% of fiber	f_{ctm}	f_{ctd}	V_C (kN)
0	11.07	7.75	18.81
1 - 25 mm	9.94	6.96	16.24
2,5 - 25 mm	10.39	7.27	17.64
1 - 35 mm	8.99	6.29	15.26

GFRP profiles of the hybrid beams corresponded from 23.72 % to 41.82 % of the average tensile failure strength of strips of the GFRP profile (Table 2).
As previously reported, the failure of the GFRP profile of all hybrid beams occurred by shearing of the concrete, which is confirmed by calculating the portion of the shear force supported only by the concrete, V_C, by the equation (12) for each volumetric percentage of fibers. In the calculation it was considered f_{ctd} being 70% of f_{ctm} (Table 4) obtained from the tests of the concrete beams. The values of fctd and V_C are presented in Table 8.

$$V_c = 0{,}6 \cdot f_{ctd} \cdot b_w \cdot d \quad (12)$$

V_C is shear force;
b_w is the concrete width of the hybrid beams;
d is the height of concrete of the beam.
It can be noticed that the shear forces of the hybrid beams, corresponding to $P_{rup}/2$ (Table 5) in bending tests, were very close to the portion of the shear force supported only by the concrete, ratifying the failure of the beam by shear.

4.2 Prototype results

Using the theory of the similarity of the physical models (Carneiro [14] and Teixeira [15]) and considering the tests results of the reduced models, one can estimate the failure values of load and vertical displacement and the masses of the sleepers in true grandeur, which are presented in the Tables 9, 10 and 11.
It is observed that the increase in the fiber volume of the sleeper reduced the mass of it. Sleepers with 1% fibers of 25 mm long, 2.5% fibers of 25 mm and 1% of fibers of 35 mm long were 0.81%, 6.68% and 10.16% lighter than the plain concrete sleepers. Compared to the prestressed concrete sleeper, the hybrid sleeper presented a weight reduction of 36.7%, 37.3%, 41.1% and 43.1%, for plain concretes, 1% fibers of 25 mm, 2.5% fibers of 25 mm and 1% fibers of 35 mm long, respectively.
The failure loads estimated to the prototype were superior to the failure load of 120 KN obtained by Bastos [2] in negative bending moment tests in the center of the concrete sleeper. The values were 114.3%, 116.4%, 134.2% and 128.6% higher than the failure load of the prestressed concrete sleeper, respectively, for plain concrete, 1% fibers of 25 mm, 2.5% fiber of 25 mm and 1% fiber of 35 mm hybrid sleepers. This happened even with the moment of inertia of the proposed hybrid sleeper corresponding to 41.6% of the moment of inertia of the usual prestressed concrete sleeper, whose cross section in the center of the sleeper is

Table 9
Specific weight and estimated mass of the sleeper prototypes

% de fiber	Beam	$\gamma_{médio}$ (kN/m³)	Prototypes	
			Mass (kg)	Mean mass (kg)
0	MODRED2	21,6	246,19	247,0
	MODRED3		248,76	–
1 - 25 mm	MODRED3	21,4	246,92	245,0
	MODRED4		241,77	–
2.5 - 25 mm	MODRED6	20,1	228,16	230,5
	MODRED7		223,74	–
1 - 35mm	MODRED3	19,4	221,90	221,9

Table 10
Prediction failure load of the sleeper prototypes

% de fiber	Beam	Prototypes	
		P_{rup} (kN)	$P_{méd\ rup}$ (kN)
0	MODRED2	255.82	257.17
	MODRED3	258.52	
1 - 25 mm	MODRED3	261.95	259.63
	MODRED4	257.31	
2.5 - 25 mm	MODRED6	271.40	281.03
	MODRED7	290.65	
1 - 35mm	MODRED3	274.37	–

Table 11
Vertical displacement on failure of the sleeper prototypes

% de fiber	Beam	Prototypes		L
		δ_{rup} (mm)	$\delta_{méd\ rup}$ (mm)	δ
0	MODRED2	15.92	16.34	L/98
	MODRED3	16.76		
1 - 25 mm	MODRED3	18.93	19.45	L/82
	MODRED4	19.96		
2.5 - 25 mm	MODRED6	19.11	19.60	L/82
	MODRED7	20.09		
1 - 35mm	MODRED3	31.36	–	L/51

presented in Figure 18. The failure loads of the prototype were estimated by subtracting from the failure load of the reduced model the weight that had to be added to the same and multiplying the value obtained by the scale factor of the applied load. The additional load of the reduced model was calculated by the equation (13) and the prototype failure load was calculated by the equation (14). Table 12 presents the failure loads and the additional loads of the reduced model and the average loads estimated for the prototypes.

$$P_{ad} = 1{,}64 \,.\, \gamma \,.\, V_{med} \quad (13)$$

Table 12
Additional load and failure load on the sleeper reduced models and prototypes (loading in the center of the sleeper)

% of fibres	Beam	Reduced model			Prototype	
		P_{rup} (kN)	$P_{méd\ rup}$ (kN)	Additional weight (kN)	P_{rup} (kN)	$P_{méd\ rup}$ (kN)
0	MODRED2	36.92	37.12	0.215	255.82	257.17
	MODRED3	37.31		0.218	258.52	
1 (25 mm)	MODRED3	37.80	37.46	0.216	261.95	259.63
	MODRED4	37.13		0.211	257.31	
2.5 (25 mm)	MODRED6	39.14	40.52	0.199	271.40	281.03
	MODRED7	41.90		0.197	290.65	
1 (35 mm)	MODRED3	39.56	39.56	0.194	274.37	274.37

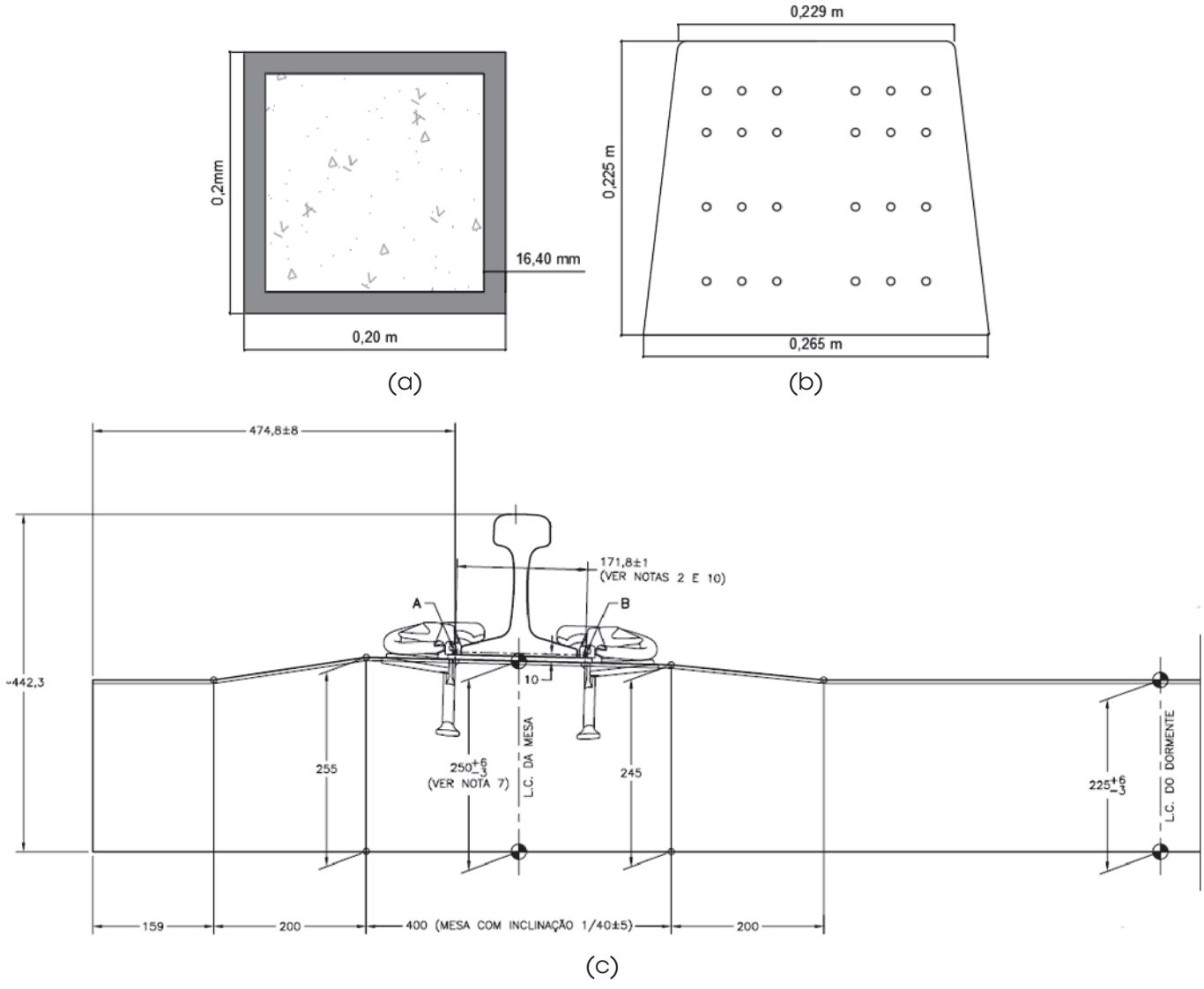

Figure 18
Transversal section in the center of the sleeper: (a) hybrid and (b) prestressed concrete and (c) half-view of the prestressed concrete sleeper DORBRÁS [19]

γ is specific weight of the hybrid beam;
V_{med} is the average volume of the prototype.

$$P_{rup\,prot} = \left(P_{rup\,mod} - P_{ad}\right).2{,}64^2 \quad (14)$$

$P_{rup\,mod}$ is the reduced model failure load;
P_{ad} is the additional load of the reduced model.
It should be emphasized that the dimensions of the cross section of the proposed hybrid sleeper (200 mm x 200 mm) are lower than the usual prestressed concrete sleeper (225 mm x 265 mm x 250 mm – smaller base x larger base x height).
The average failure vertical displacement estimated for sleeper prototypes varied from L/51 to L/82. These values were lower than the L/41 value obtained by Muttashar [16], indicating a good performance of the proposed hybrid sleeper.

5. Conclusion

The addition of fibers to the concrete increased a little the failure load of the beams and allowed greater tensile stresses on the lower edge of the GFRP profile, suggesting greater elongation of the concrete with fibers in relation to the plain concrete until the failure.
The addition of polyolefin fibers also contributed to the reduction of the widths of the cracks on the concretes with 2.5% by volume of fibers of 25 mm long and 1% by volume of fibers of 35 mm long.
In the tests with loading at the center of the sleeper, the failure of all the hybrid beams occurred on the lower edge of the hybrid sleeper due to the rupture of the concrete by shear followed by the rupture of the GFRP profile parallel to the fibers. In none of the tests occurred the rupture of the compressed concrete.
The vertical displacements at the proposed sleeper ranged from L/101 to L/51, having been slightly lower than the values obtained by Gibson [5] and approaching the values obtained for wood sleepers, as mentioned by this same author.
The sleepers proposed with 1% fibers of 25 mm, 2.5% fibers of 25 mm and 1% of fibers of 35 mm long were 0.81%, 6.68% and 10.16% lighter than the plain concrete sleeper, respectively. The average failure loads of the hybrid sleepers were 114.3%, 116.4%, 134.2% and 128.6% higher than the failure load of the prestressed concrete sleeper, respectively, for plain concrete, 1% fibers of 25 mm, 2.5% fibers of 25 mm and 1% fibers of 35 mm long on the negative bending moment tests in the center of the sleeper.
Finally, it can be concluded that the performances of the sleepers proposed were quite satisfactory in terms of strength and weight, comparing with prestressed concrete sleepers, being a technical viable alternative. As recommendation for future works, the authors suggest the conduction of fatigue tests and tests of a true grandeur hybrid sleeper.

6. References

[1] PLANETA FERROVIA - Bitolas Ferroviárias, 2014. Available in: http://planetaferrovia.blogspot.com/2014/01/bitolas-ferroviarias.html., Access in July 2018.

[2] BASTOS, S, S, Análise experimental de dormentes de concreto protendido reforçado com fibras de aço, Tese de Doutorado, Escola de Engenharia de São Carlos, São Carlos, SP, Brasil, 1999.

[3] TRINDADE, E. J. Análise sobre a utilização de dormentes de concreto como solução alternativa para a via permanente na MRS Logística S. A. Trabalho Final de Curso, Programa de Especialização de Transporte Ferroviário, Instituto Militar de Engenharia, Rio de Janeiro, 2012.

[4] DEPARTAMENTO NACIONAL DE INFRAESTRUTURA DE TRANSPORTES - DNIT, PIM - Procedimento de Inspeção de Material, Dormente de Aço para Via Férrea. Available in: www.dnit.gov.br/...e...para.../PIM%20016%20-%20Dormente%20de%20Aço.pdf, acesso em abril de 2018.

[5] GIBSON, R. F., Principles of Composite Material Mechanics, Ed, McGraw-Hill, 1994.

[6] FERDOUS, W., KHENNANE, A., KAYALI, O., Hybrid FRP-concrete railway sleeper, University of ´New South Wales, Canberra, Australia, 2013.

[7] MUTTASHAR, M., MANOLO, A., KARUNASENA, W., LOKUGE, W., Influence of infill concrete strength on the flexural behaviour of pultruded GFRP square beams, Composite Structures, v. 145, p. 58-67, 2016.

[8] MUTTASHAR, M., MANOLO, A., KARUNASENA, W., LOKUGE, W., Flexural behaviour of multi-celled GFRP composite beams with concrete infill: Experiment and theoretical analysis, Composite Structures, v. 159, p. 21-33, 2017.

[9] GASPAR, D. H., CARNEIRO, L. A. V., TEIXEIRA, A. M. A. J., Estudo de placas de concreto com fibras de aço e de poliolefina submetidas a impacto balístico. REVISTA MILITAR DE CIÊNCIA E TECNOLOGIA, v. XXXIII, p. 57-62, 2016.

[10] ALBERTI, M. G., ENFADAQUE, A., GÁLVEZ, J.,C., AGRAWAL, V., Reliability of polyolefin fibre reinforced concrete beyond laboratory sizes and construction procedures, Composite Structures, v. 140, p. 506-524, 2016.

[11] ALBERTI, M. G., ENFADAQUE, A., GÁLVEZ, J. C., AGRAWAL, V., Fibre distribution and orientation of macro-synthetic polyolefin fibre reinforced concrete elements, Construction and Building Materials, v. 122, p. 505-517, 2016.

[12] ASSOCIAÇÃO BRASILEIRA DE NORMAS TÉCNICAS. Dormente de concreto - Projeto, materiais e componentes. - NBR 11709, Rio de Janeiro, 2015.

[13] AMERICAN RAILWAY ENGINEERING AND MAINTENANCE ASSOCIATION. Manual for Railway Engineering - Concrete Ties. - AREMA, v.1, cap 30, 2016.

[14] CARNEIRO, F. L., Análise dimensional e teoria das semelhanças e dos modelos físicos, Rio de Janeiro, Editora UFRJ, 256p, 1996.

[15] TEIXEIRA, A. M. A. J., Ponte desmontável em material compósito de fibra de vidro, Tese de D.Sc., COPPE/UFRJ, Rio de Janeiro, RJ, Brasil, 2007.

[16] AMERICAN SECTION OF THE INTERNATIONAL ASSOCIATION FOR TESTING MATERIALS. Standard Test Methods for Rubber Products - Chemical Analysis. - ASTM D297, Philadelphia, PA, 2013.

[17] AMERICAN SECTION OF THE INTERNATIONAL ASSOCIATION FOR TESTING MATERIALS. Standard Test Method for Tensile Properties of Polymer Matrix Composite Materials. - ASTM D3039/D3039M, Philadelphia, PA, 2008.

[18] ASSOCIAÇÃO BRASILEIRA DE NORMAS TÉCNICAS, NBR 5739: Concreto – Ensaio de compressão de corpos-de-prova cilíndricos, Rio de Janeiro, 1994.

[19] COMPANIA BRASILEIRA DE DORMENTES – DORBRÁS. Available in: http://dorbras.com.br. Acesso em agosto 2016.
[20] MUNDO DAS TRIBOS, Dormente de Madeira. Rio de Janeiro. Available in: <http://www.mundodastribos.com/dormentes-de-madeira-precos.html> Acesso em jan de 2017.
[21] PANDROL, Track Report, France, 1996, Available in: http://www.pandrol.com/download/pandrol-track-report-1996/. Acesso em: maio de 2017.